BBAA VI International Colloquium on:
Bluff Bodies Aerodynamics & Applications
Milano, Italy, July, 20-24 2008

MODELING OF POLLUTION DISPERSION AROUND A CUBIC OBSTACLE

Jalal Abedi and Mohammad Omidyeganeh

Department of Chemical and Petroleum Engineering, University of Calgary, 2500 University Drive, NW, Calgary, AB T2N 1N4, Canada
e-mails: jabedi@ucalgary.ca, momidyeg@ucalgary.ca

Keywords: large eddy simulation (LES), Smagorinsky-Lilly sub-grid scale (SGS) model, finite volume (FV) methods, TVD scheme, pollution dispersion.

Abstract. *A code has been developed in C++ to solve the Navier-Stokes, continuity, and mass transfer equations using large eddy simulation (LES) for the turbulent flow. The pollution dispersion around a cube was investigated. The pollutant source was placed on the ground, right behind the cube. In the code, the finite volume (FV) formulation applied on the staggered grid arrangement for a structured mesh system. Smagorinsky-Lilly sub-grid scale (SGS) model was used. The discretisation scheme for all terms except the convection terms in the momentum equations, which adopts a TVD scheme, was the central difference scheme. The PISO algorithm showed faster convergence behavior than the other well known algorithm such as SIMPLE. The pollution dispersion behind the cube has been obtained assuming that the molecular diffusivity is dominant and neglecting the buoyancy effects.*

1 INTRODUCTION

There is a growing concern about air pollution in urban environments due to the dispersion of chemical and biological agents. It is now generally recognized that many of the substances directly emitted by vehicles, or accidentally released by different kinds of sources, into the ambient air represent a serious hazard for human health (Ref. [4], Ref. [10], and Ref. [2]). To assess the magnitude of the problem, accurate prediction of contaminant dispersion in urban area is needed.

The wind flow patterns in an urban area strongly affect the dispersion of pollutants around the buildings which is a growing concern in urban environment. The air flow is influenced by various factors, such as the geometry, arrangements of the buildings, the wind directions and the upstream terrain conditions. With a steady growth in computer technology, computational fluid dynamics (CFD) has emerged as an effective tool to establish better understanding of the wind flow around buildings. Nowadays, high performance computing (HPC) provides cluster-based supercomputers for computing applications to make CFD analysis as fast as possible.

CFD codes are structured around numerical algorithms that can tackle fluid flow problems. In order to provide easy user access, most CFD codes include sophisticated input and output interfaces. Hence, they contain three main elements: the pre-processor, the solver, and the post-processor. There are several approaches to computer prediction of flows; the most popular ones involve the use of Reynolds-averaged Navier-Stokes (RANS) equations with a variety of turbulence models. While these are much cheaper than large eddy simulations, no single model has proven capable of predicting a wide variety of complex flows, especially when information about the fluctuating part of the flow is required (Ref. [15]).

These considerations have led to interest in large eddy simulation (LES), in which the large-scale motions are computed explicitly, while the small- or sub-grid-scale motions are modeled. The fundamental rationale behind LES is that large eddies are the ones responsible for most of the mass, momentum and energy transport. These large eddies are strongly dependent on geometry, whereas the smaller eddies are more universal and, thus, easier to model. As the grid resolution increases, the importance of the small eddies diminishes, and LES becomes a direct numerical simulation (DNS). Unfortunately, flows that are of interest to engineering applications (high Reynolds number and complex geometry) are not amenable to DNS, due to prohibitive memory and computational requirements.

The primary objective of our study is the development of a code to investigate the flow past buildings and the dispersion of pollutants due to the local geometry. Most of the applications discussed here are focused on a cube, since it is the simplest idealization of a building and has, therefore, been used most frequently, both in experiments and testing calculation procedures for the flow around buildings.

The lack of integrated and fully concerned commercial software for urban area pollution dispersion, which would be capable of considering features of city areas and meteorological data, encouraged us to write our own code. An advantage of this code is that, because the software is fully understood by the researchers, they are able to modify any part of the code. The C++ code that has been developed so far is an initial attempt and covers a model in LES with limited but outstanding capabilities.

The study of pollution entrainment in urban areas with different arrangements of bluff bodies is a new branch of environmental engineering. Since the analysis of flow field in complex geometries is very costly, the simple pollution dispersion around a cube mounted on a surface is still under investigation. The entrainment of pollutants into and out of the recirculation cavity is controlled by both advection and diffusion processes. Another important factor affecting the entrainment of pollutants into and out of the wake region is the unsteadiness of the wake caused by the shedding of corner vortices.

Mavroidis (Ref. [7]) conducted an experimental investigation on the plume dispersion around single isolated obstacles. Dispersion around a single cube was mainly investigated in the wind tunnel; and, the results confirm, in general, the findings of the field trials. However, comparisons between wind tunnel and field results clearly show that the plume is more dispersed in the field, which is attributable to the effect of additional wind meander occurring in the atmosphere; whereas centerline concentrations were found to be higher in the wind tunnel.

A brief review of the modeling of air quality in street canyons (the spaces between buildings) has been conducted by Vardoulakis (Ref. [17]). Gaussian plume models, operational street canyon models, CFD models, and reduced-scale models were presented and compared with each other in different aspects. For the selection of the appropriate dispersion model, capabilities, underlying assumptions and limitations of the available resources should be considered. Although models vary greatly in terms of complexity, simple and advanced models can be both useful in different air quality applications (Ref. [1]). For regular purposes, using a simple screening model seems reasonable. While for quick air quality surveys and traffic planning, simulations with a simple model might be more feasible. On the other hand, air quality monitoring network design may require both parametric modeling for an initial selection of the streets to be implemented and CFD simulations to identify representative locations within these streets (Ref. [17]).

Most of the empirical relations derived so far to account for building effects on plume dispersion are not designed for complex situations. The relations are usually based on simple modifications to the Gaussian plume diffusion model. Gaussian plume models are routinely applied in studies of environmental impact, due to their ease of application, acceptable level of accuracy, and a long history of application. They work well in situations that have uncomplicated transport and diffusion between source and receptors. Most of these models require only the mean wind at emission height, emission rate, source-receptor distance, plume rise, and atmospheric stability.

A good review on the basic equations used by meteorological models has been done by Pielke and Nicholls (Ref. [12]), where empirical and numerical modeling was discussed. An analytical method that provides a very simplified prediction of mean velocity, turbulence intensity, mean temperature and mean concentration of pollutants in the wake region downwind of buildings, was reviewed by Peterka (Ref. [11]).

The processes associated with the flow past structures in the urban boundary layer are so complex and subject to many different parameters. In general, numerical modeling based on solving the governing partial differential equations, such as momentum, continuity, mass and energy equations, is required for the various flow quantities. Powerful numerical techniques, as well as high capacity computers, are necessary; and, there are various possibilities of treating turbulence in numerical calculations.

Despite progress since the first LES by Deardorff (ref. [3]), there was not much application of LES to engineering flows for quite a long time, mainly because it requires considerable computing resources and but also due to lack of good models for the small scales. The unsteady turbulent flow field around a cubic model was first simulated by Murakami and Mochida (Ref. [8]) by means of LES. Calculations obtained by Rodi (Ref. [13]) with a variety of LES and RANS methods shows that LES is clearly more suited than RANS methods and have great potential for calculating complex flows.

The finite volume (FV) method was adopted to apply LES to the Navier-Stokes equations in the 3D geometry. The code was written entirely in the C++ language except the visualization of the results where the Tec Plot commercial software was used.

2 GOVERNING EQUATIONS

The governing equations consist of the principles of conservation of mass and momentum in addition to mass transfer equation. All quantities become non-dimensionalized using a length scale, H_b (for example for a flow past a cube, the length scale is the dimension of the cube), the velocity scale U_b (the velocity of the laminar flow at the inlet of the domain at the height of the cube for all cases), and the concentration scale C_e (the pollution source emission concentration).

The filtered continuity and Navier-Stokes equations using top-hat filter for an incompressible flow are:

$$\frac{\partial u}{\partial x}+\frac{\partial v}{\partial y}+\frac{\partial w}{\partial z}=0 \tag{1}$$

$$\frac{\partial u}{\partial t}+u\frac{\partial u}{\partial x}+v\frac{\partial u}{\partial y}+w\frac{\partial u}{\partial z}=-\frac{\partial P}{\partial x}+\frac{1}{\mathrm{Re}}\left(\frac{\partial^2 u}{\partial x^2}+\frac{\partial^2 u}{\partial y^2}+\frac{\partial^2 u}{\partial z^2}\right) \tag{2}$$

$$\frac{\partial v}{\partial t}+u\frac{\partial v}{\partial x}+v\frac{\partial v}{\partial y}+w\frac{\partial v}{\partial z}=-\frac{\partial P}{\partial y}+\frac{1}{\mathrm{Re}}\left(\frac{\partial^2 v}{\partial x^2}+\frac{\partial^2 v}{\partial y^2}+\frac{\partial^2 v}{\partial z^2}\right) \tag{3}$$

$$\frac{\partial w}{\partial t}+u\frac{\partial w}{\partial x}+v\frac{\partial w}{\partial y}+w\frac{\partial w}{\partial z}=-\frac{\partial P}{\partial z}+\frac{1}{\mathrm{Re}}\left(\frac{\partial^2 w}{\partial x^2}+\frac{\partial^2 w}{\partial y^2}+\frac{\partial^2 w}{\partial z^2}\right) \tag{4}$$

$$\frac{\partial C}{\partial t}+u\frac{\partial C}{\partial x}+v\frac{\partial C}{\partial y}+w\frac{\partial C}{\partial z}=D\left(\frac{\partial^2 C}{\partial x^2}+\frac{\partial^2 C}{\partial y^2}+\frac{\partial^2 C}{\partial z^2}\right)+\dot{n} \tag{5}$$

where u, v, w, P, and Re are the velocities in the x, y, and z-direction, absolute pressure, and Reynolds number ($\mathrm{Re}=\rho U_b H_b/\mu$). C is the concentration of pollutant, Dt is the effective diffusivity of mass, and $\dot{N}$ is the source emission rate. For simplicity define the velocity vector, $\vec{u}$, that has the u-, v-, and w-components. The effective diffusivity of mass should be calculated by Eq. (6) where ν_t is the turbulent kinematic viscosity (or ν_{SGS} in our case that we adopt LES) and ScT is the turbulent Schmidt number and equal to 0.77 (Ref. [20]). But for the first try, the molecular diffusivity is just considered.

$$D_t=\nu_t/Sc_T \tag{6}$$

Second terms on the left hand side of Eqs. (2)-(4) were treated by defining sub-grid-scale stresses: $\tau_{ij}=\rho\overline{u_i u_j}-\rho\overline{u}_i\overline{u}_j$. Smagorinsky (Ref. [16]) suggested that, since the smallest tur-

bulent eddies are almost isotropic, we expect that the Boussinesq hypothesis might provide a good description of the effects of the unresolved eddies on the resolved flow.

$$\tau_{ij} = -2\mu_{SGS}\bar{S}_{ij} + \frac{1}{3}\tau_{ii}\delta_{ij} = -\mu_{SGS}\left(\frac{\partial \bar{u}_i}{\partial x_j} + \frac{\partial \bar{u}_j}{\partial x_i}\right) + \frac{1}{3}\tau_{ii}\delta_{ij} \tag{7}$$

The isotropic part of the SGS stress in Eq. (7) was absorbed into the large scale pressure to avoid dealing with unknown variables and solve them altogether by pressure.

$$\tau_{ij}{}^{a} = \tau_{ij} - \frac{1}{3}\tau_{ii}\delta_{ij} = -\mu_{SGS}\left(\frac{\partial \bar{u}_i}{\partial x_j} + \frac{\partial \bar{u}_j}{\partial x_i}\right) \tag{8}$$

The Smagorinsky-Lilly SGS model builds on Prandtl's mixing-length model and assumes that we can define a kinematic SGS viscosity, $\nu_{SGS} = \mu_{SGS}/\rho$, which can be described in terms of one length scale and one velocity scale. Since the size of the SGS eddies is determined by the details of the filtering function, the obvious choice for the length scale is the filter cutoff width Δ. In 3D computations with grid cells of different length Δx, width Δy and height Δz the cutoff width is often taken to be the cube root of the grid cell volume $\Delta = \sqrt[3]{\Delta x \Delta y \Delta z}$. The velocity scale is expressed as the product of the length scale and the average strain rate of the resolved flow, $\Delta \times |\bar{S}|$ *where* $|\bar{S}| = \sqrt{2\bar{S}_{ij}\bar{S}_{ij}}$ and the local rate of strain of the resolved flow are $\bar{S}_{ij} = \frac{1}{2}\left(\frac{\partial \bar{u}_i}{\partial x_j} + \frac{\partial \bar{u}_j}{\partial x_i}\right)$.

$$\mu_{SGS} = \rho(C_{SGS}\Delta)^2|\bar{S}| \tag{9}$$

Different values of C_{SGS} have been imposed so far (Ref. [5] and Ref. [13]); however $C_{SGS}=0.1$ is used more often in the commercial software. The difference in C_{SGS} values is attributable to the effect of the mean flow strain or shear.

3 NUMERICAL METHOD

Simple structured grids are used in this code. Due to the large changes in velocity and pressure next to the wall and around the buildings, refined grids are adopted with a stretch ratio by distance from the walls. A large ratio of grid stretching often leads to numerical oscillation due to the grid size differences between two neighboring grids. The Reynolds number of the flow field treated in atmospheric boundary is usually large which generally requires fine grid resolution. Turbulence modeling makes it possible to use a relatively coarse grid in the domain except near the solid walls of bluff bodies where high prediction accuracy is needed. In order to apply the non-slip boundary condition accurately, it is preferable to set the first grid point below $x_n{}^{+}=1$ ($x_n{}^{+} = u^* x_n/\nu$, where u^* is the friction velocity, x_n is the distance from the wall, and ν is kinematic viscosity). For example, in the flow field around a square cylinder (with side length of D) at $Re=22000$ the real length corresponding to $x_n{}^{+}=1$ is about $D/1000$ (Ref. [6]).

The code uses a simple stretching procedure where the grid space of an arbitrary grid to the smaller neighbor grid space is equal to the ratio ($\Delta x_n / \Delta x_{n-1} = r$). Thus the number of grids of a distance equal to L with ratio r and the finest resolution dx is given by Eq. (10).

$$n = \left\lfloor \ln\left[1 + L\frac{r-1}{d}\right] \Big/ \ln r \right\rfloor \tag{10}$$

A computational mesh used in the simulation for a cube flow is shown in Fig. (1).

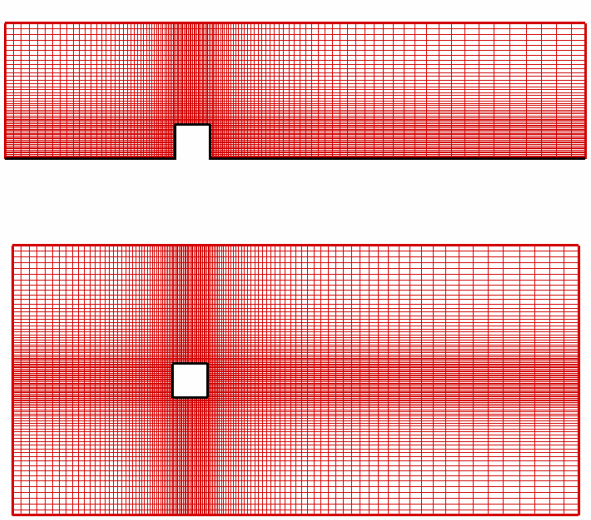

Figure 1: Computational mesh for the flow past a cubic obstacle 3D mesh around a cube mounted on a surface

All the equations are discretized based on the finite volume method and a staggered Cartesian grid. In the present research, the code uses second-order accuracy, which means each discretized term in the equation has a truncation error proportional to the square of grid spacing and time marching. This implies that the global truncation error is first-order, and the method is still consistent. Many discretization schemes have been proposed, so far, for the equations that contain convection and diffusion terms the basic upwind scheme is the most stable and unconditionally bounded scheme, but the order of accuracy is low (first-order). Higher order schemes such as central differencing and QUICK can cause oscillations in the results especially when the Peclet number is high. These higher order schemes give unrealistic physical turbulence energy and rates of dissipation (Ref. [18]). Total variation diminishing (TVD) schemes are designed to counteract with the oscillation by adding an artificial diffusion fragment or by adding a weighting towards upstream contribution. Discretization of the diffusion terms in the governing equations using the central differencing is standard and does not require any further consideration.

The general form of TVD schemes of the east face value φ_e is shown in Eq. (11), which uses the notations in Fig. (2) with flow in the positive x-direction.

$$\phi_e = \phi_P + \frac{1}{2}\psi(r)\left(\phi_E - \phi_P\right) \tag{11}$$

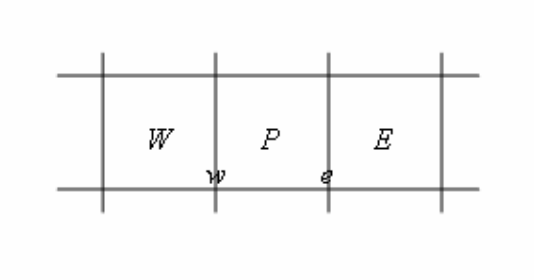

Figure 2: grid notations in the *x*-direction

where $r = \left(\frac{\phi_P - \phi_W}{\phi_E - \phi_P} \right)$.

By introducing TVD schemes, the goal was to find a stable scheme with a higher-order of accuracy without wiggles. In the present research, due to simplicity, the UMIST function was used.

$$\psi(r) = \max\left[0, \min\left(2r, (1+3r)/4, (3+r)/4, 2\right)\right] \tag{12}$$

Fully implicit method was adopted in the code. Therefore an inner iteration loop was needed to get the accurate results caused by the nonlinearity of the equations. Fully implicit second-order upwind schemes used in the discretization method guarantees the stability of the numerical method. For the time marching term in equations, the Adam-Bashforth second-order scheme was used.

The choice of the time step Δt was governed by several criteria. The stability limit of the time advancement scheme plays no role in this code due to the stable method. However, physical considerations limit the time step selection. In order to predict the turbulence statistics correctly all contributions to turbulence must be resolved and captured. The turbulence fluctuations cannot be satisfied if the computational time step becomes larger than the Kolmogorov time scale (ν/u_τ^2 where u_τ is called frictional velocity). In the present work it was found that the Courant-Fredrichs-Lewy (CFL) limit (shown in Eq. (13)) of *1* produces a time step much smaller than the Kolmogorov time scale.

$$CFL = \Delta t \left(\frac{|u|}{\Delta x} + \frac{|v|}{\Delta y} + \frac{|w|}{\Delta z} \right)_{\max} \tag{13}$$

The no-slip boundary condition was used on all solid walls for all simulations. The free slip boundary condition was used for outflow, where, it was surmised that the length of the domain was long enough that the effect of the bodies are vanished and the fully developed condition was applicable. The symmetry boundary condition was used in the spanwise direction, which, means the normal velocity is zero and the changes in other velocity components are zero.

In wind engineering problems, a high Reynolds number is usually applicable which makes it very difficult to use the no-slip boundary condition at solid walls. Therefore, some wall function should be adopted as a macroscopic boundary condition which is absolutely necessary in this kind of atmosphere problems. Wengle and Werner (Ref. [19]) proposed a wall boundary condition which assumes that at the grid points closest to the wall, the instantaneous

velocity components tangential to the wall are in phase with the instantaneous wall shear stress components, and the instantaneous velocity distribution is assumed to follow the linear law of the wall.

$$|\tau_{ub}| = \frac{2\mu|u_P|}{\Delta z} \qquad for \qquad |u_P| \le \frac{\mu}{2\rho\Delta z} A^{\frac{2}{1-B}} \tag{14.a}$$

$$|\tau_{ub}| = \rho\left[\frac{1-B}{2} A^{\frac{1+B}{1-B}} \left(\frac{\mu}{\rho\Delta z}\right)^{1+B} + \frac{1+B}{A}\left(\frac{\mu}{\rho\Delta z}\right)^{B} |u_P|\right]^{\frac{2}{1+B}} \qquad o.w. \tag{14.b}$$

The proposed function was transferred to a non-dimensional form and was used in the code. Δz is the distance of the wall to the closest point in the normal direction, with $A=8.3$ and $B=1/7$. The wall function was not applied explicitly in the equations. Strain calculation uses this function to get the shear stresses near the walls and implicitly has an interaction in the momentum equations.

Inflow boundary conditions are very challenging since the inlet flow properties are convected downstream, and inaccurate specification of the inflow boundary condition can strongly affect simulation quality. Using an accurate inlet flow was impossible due to lack of exact measurements in real world. One of the most applicable options was to use a non-turbulent mean velocity profile measured experimentally at the inlet. To have a fully turbulent flow at the upstream of the obstacles of a very large domain was required to ensure that the turbulence is fully developed before it reaches the body. This method greatly increases the computational time and was not currently efficient for this code. Another idea was to superimpose random perturbations with the correct turbulence intensity into the mean profile. In the present work the time-averaged streamwise velocity component was set to obey the power law expressed as $z^{1/4}$ in the non-dimensional form (for the half of the channel height where a symmetric profile was adopted for the other half). This expression represents the flow of atmospheric boundary layer conditions while other velocity components are assumed to be zero. The value of ¼ corresponds to the wind tunnel experiment done by Murakami and Mochida (Ref. [9]).

Another problem in turbulent flow simulation is the generation of the initial condition which must contain all the details of the initial three-dimensional velocity field. Since coherent structures are an important component of the flow, it is really difficult to construct such a field. Furthermore, data from experiments or a reliable direct numerical simulation (DNS) are not usually available. The effects of initial conditions are typically remembered by the flow for a considerable time. Thus the initial conditions have a significant effect on the results or at least consume significant computational time to disappear. In the present work there was not such a data for initial conditions and as a result a zero value was used for all variables and a great deal of time was spent to get a reliable results that was not been affected by the initial condition.

The mass transfer equation is not coupled with fluid flow equations as long as the heat transfer equation is neglected. In the present work, a constant temperature was assumed and as a result there were no heat transfers in the domain. Therefore, the mass transfer equation can be solved right after the fluid flow is obtained at a specific time.

The main body of the code was a method that should be used to solve coupled equations in the time step. The most common methods in the literature are SIMPLE, SIMPLER, SIMPLEC, and PISO. The code is capable of switching between the two algorithms SIMPLE and PISO. PISO may be seen as an extended SIMPLE algorithm with one extra corrector step. The PISO algorithm requires additional memory storage due to the second pressure correction equation. It also needs under-relaxation to stabilize the calculation process. Although this method results in significant computational effort in comparison with the SIMPLE algorithm it has been found that the method is fast and efficient. For the present work the central processing unit (CPU) time for a single time step reduced by a factor of 8 compared with the previously discussed standard SIMPLE algorithm.

The selection of solver for algebraic equations is changed case by case and in the present work we use SIP (Strongly Implicit Procedure) for momentum equations and CG (Conjugate Gradient) for pressure correction equations.

All cases run on the WestGrid clusters (Glacier).

4 RESULTS

In the present work, the code described above was used to simulate the pollution dispersion around a cube mounted on a surface in the atmosphere boundary layer.

The performance of the developed code was already examined for the air flow patterns by comparing the numerical results with the wind tunnel experiments conducted by Murakami and Mochida (Ref. [9]). In addition, effects of a few parameters were observed for the flow past a cube in the atmosphere boundary layer.

Here the pollution dispersion results with the specified assumptions described above are presented. The same results as the experimental data were not expected, because the cases used in the simulations were different than reality. Despite the differences existed for the air flow problem such as the laminar inflow boundary condition, the simplified diffusivity parameter plays a major role in the dispersion results. Therefore, the simulation results are illustrated and qualitatively assessed.

A cube with dimension H_b is mounted on a surface in the computational domain with streamwise length of $17H_b$, spanwise length of $8H_b$ and height of $4H_b$. The cube is placed $5H_b$ down the inlet and at the middle of the spanwise direction ($3.5H_b$ distance to each side). Table 1 gives enough information on the case used in the simulation. The Reynolds number is calculated by $\mathrm{Re} = \dfrac{\rho U_b H_b}{\mu}$ where U_b is the velocity at the height of the obstacle at the inlet. The time step is 0.005 non-dimensional (using the length and velocity scales, H_b and U_b). The terms (x_p, y_p) represent the place of the cube in the x and y coordinates.

Table 1: Cases of LES performed for the cube flow in atmosphere boundary layer

Case	(x_p,y_p)	$(\Delta x_{min},\Delta y_{min},\Delta z_{min})$	$(\Delta x_{max},\Delta y_{max},\Delta z_{max})$	(n_x,n_y,n_z)	n	Re
1	(5.5,4)	(0.04,0.04,0.04)	(1.157,0.467,0.397)	(74,63,43)	200466	10000

The approaching flow was laminar, while the inlet flow of the experiment performed by Zhang (Ref. [20]) was turbulent; therefore, the flow pattern was different in these two cases. Consequently, similar results were not expected since the pollutant release point was behind the cube on the ground which was a challenging zone of the turbulent flow that differs totally for both cases.

The streamlines for the flow in the atmosphere boundary layer, at the centerline vertical plane of case 1 (Fig. (3)), show that the flow adjacent to the lee face of the cube was less upward and more backward. Pollutants released within a large recirculating cavity may be expected to be mixed rapidly throughout the cavity's volume. However, no inlet flow was considered for the point source weakening the mixing phenomenon. In addition, due to small flow velocity around this point, the mixing process needed significant computational time to be accomplished.

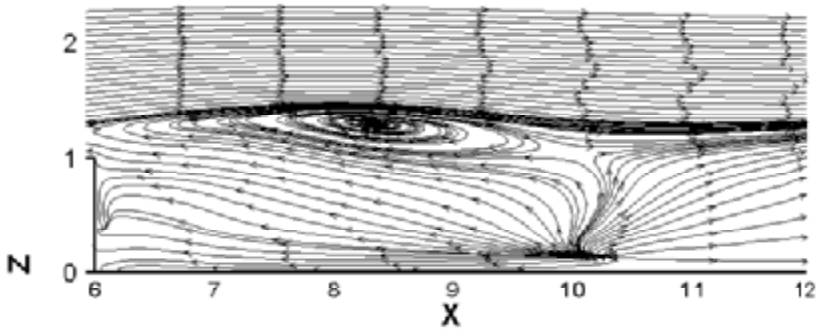

Figure 3: Time-averaged streamlines behind the cube at the central vertical plane

Figure 4 displays the longitudinal ground-level concentration profile. The normalized concentration is defined as Eq. (15). Where, Q is the source pollutant release rate in terms of 'concentration × volume/time'.

$$C = cU_b H_b^{\,2} / Q \tag{15}$$

The pollutant concentration significantly decreased directly downwind of the pollutant source. This was due to the large reverse flow and the large vortex behind the building which prohibited the compilation of pollutants in this area.

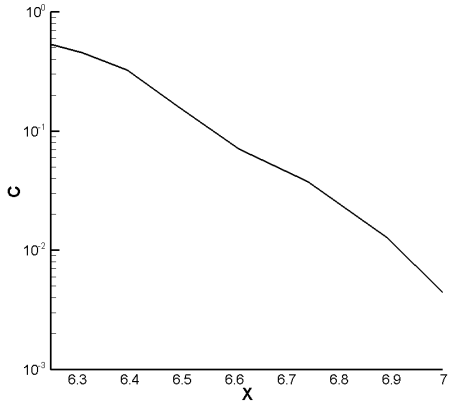

Figure 4: Normalized ground-level concentration along the source centerline downwind of the cube

The normalized vertical concentration profile right behind the cube at centerplane through the cube is shown in Fig. (5). This profile verifies the earlier discussion that the pollutant is not being raised very much. The concentration was almost zero next to the wall above the height of $0.06H_b$.

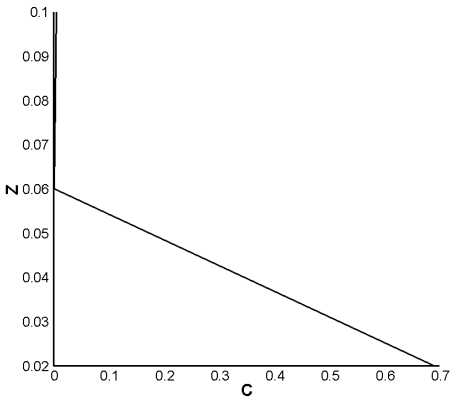

Figure 5: Normalized vertical concentration profile at $0.1H_b$ downstream from the building at the centerplane through the cube

Fig. (6) displays the normalized lateral ground-level concentration profile at $0.1H_b$ downwind of the cube. The symmetric profile was also measured in the experiment conducted by Zhang (Ref. [20]).

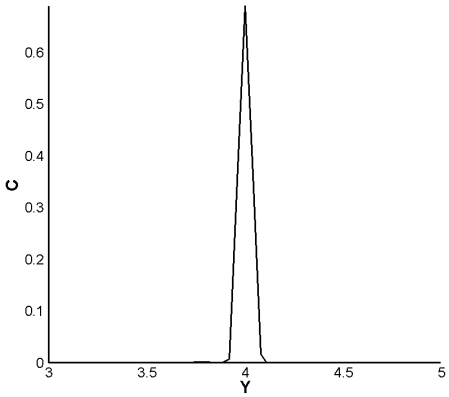

Figure 6: Normalized lateral ground-level concentration profile at $0.1H_b$ downstream from the cube

The calculations performed by Zhang (Ref. [20]) could not capture the profile appropriately. Experiments showed one maximum point, however the simulation obtained two maximum points in the concentration profile. These results also showed two maximum points far downwind from the cube as illustrated in Fig. (7).

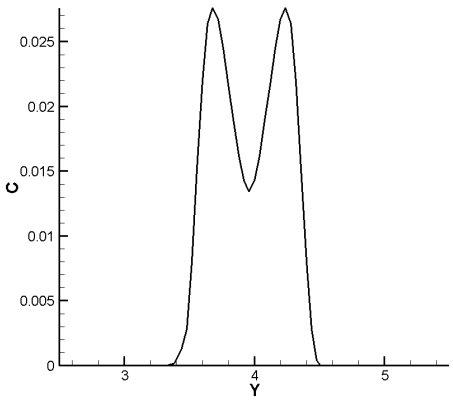

Figure 7: Normalized lateral ground-level concentration profile at $6H_b$ downstream from the cube

Fig. (8) shows snapshots taken from the concentration field every one minute from the horizontal plane through the center of the cube.

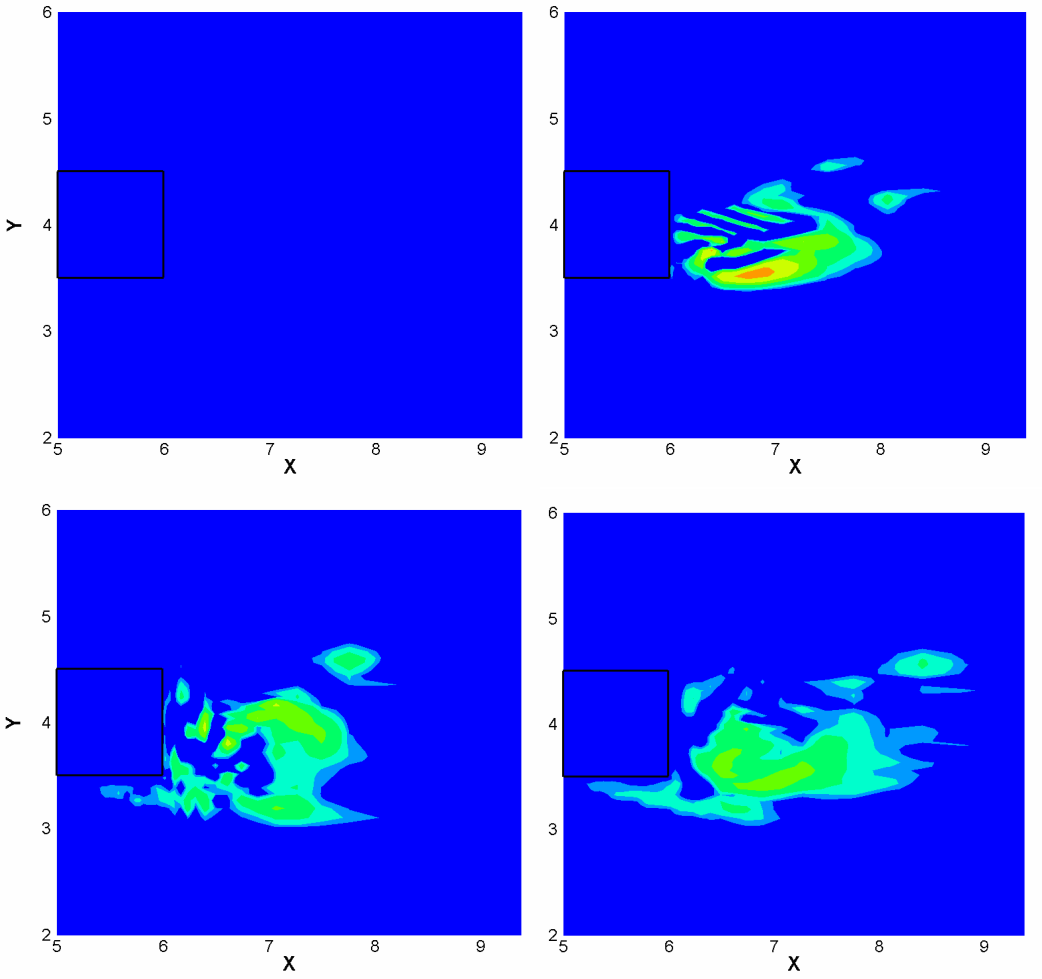

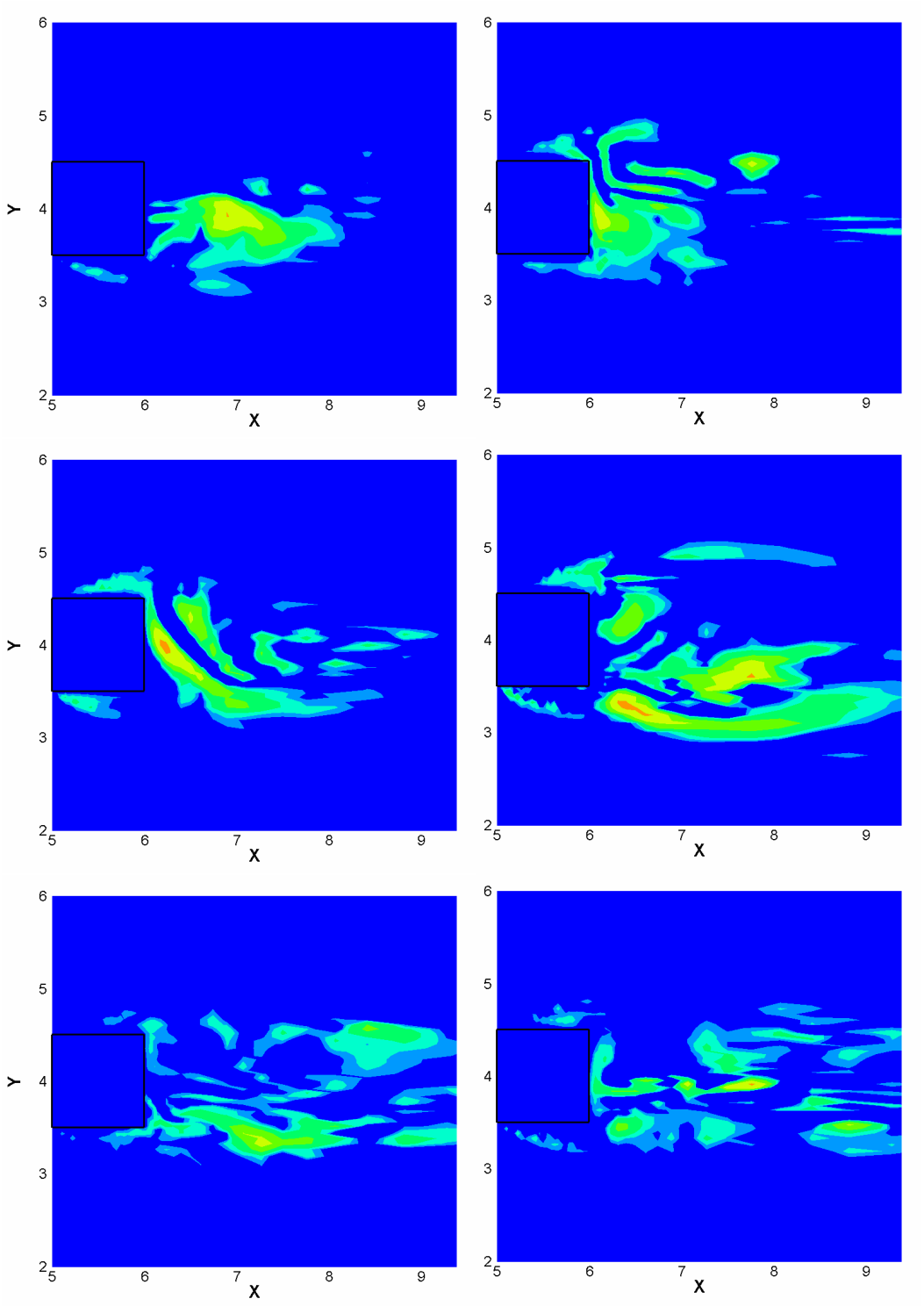
Y
X
2
3
4
5
6
5
6
7
8
9

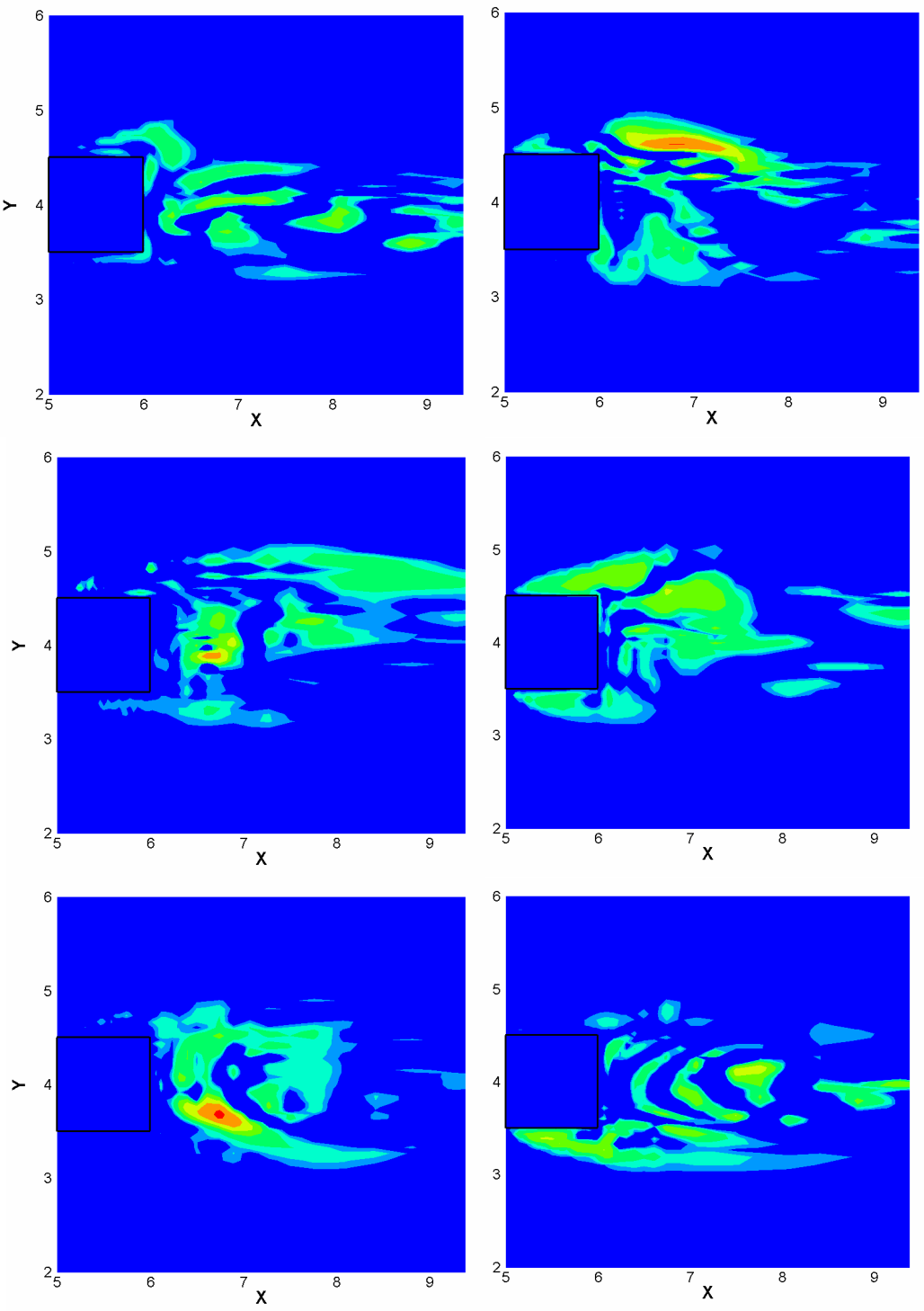
Y
X
2
3
4
5
6
7
8
9

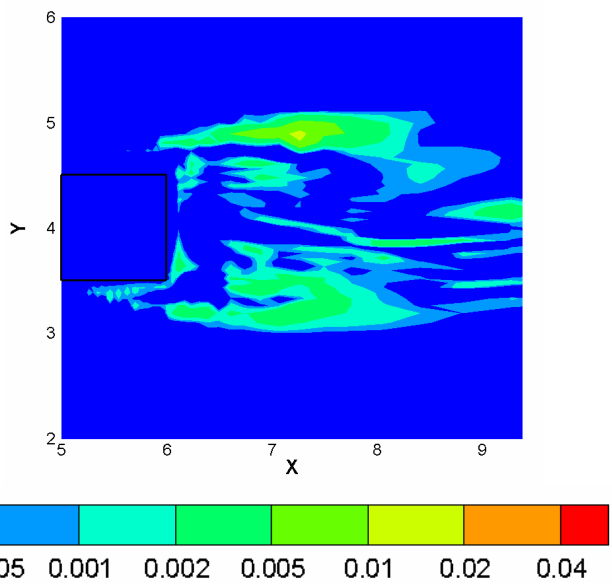

Figure 8: Snapshots of Concentration contours at horizontal plane through the center of the cube taken every 1 minute

5 CONCLUSIONS

It can be concluded from all the results presented above that the developed code in C++ shows a good capability to capture the pollution dispersion around buildings. However, more investigations and modifications are needed to improve the code in an appropriate way to solve more realistic problems with fewer simplifications. Evaluation of the simulation results of pollutant dispersion around a cube in the atmospheric boundary layer was not performed completely. The primary results obtained based on big simplifications such as domination of the molecular diffusivity over the turbulent diffusivity showed reasonable behavior. However, the code for the pollution dispersion was applied for a case in the problem of flow around a cube in atmospheric boundary layer which was not the best case but it was the simplest case. Overall, the concentration patterns illustrated in this work shows reasonable trends was expected by the experiments.

6 ACKNOWLEDGEMENT

This research has been supported by the Natural Sciences and Engineering Research Council of Canada (NSERC) and we are grateful for the financial support. The authors would also like to thank WestGrid Canada for their computational resources.

REFERENCES

[1] Berkowicz, R., 'Modeling street canyon pollution: model requirements and expectations', International Journal of Environment and Pollution 8 (3–6), 609–619, 1997.

[2] Dab W, Segala C, Dor F, Festy B, Lameloise P, Le Moullec Y, Le Tertre A, Medina S, Quenel P, Wallaert B, Zmirou D, 'Pollution atmosphérique et sante : Corrélation ou causalité ? Le cas de la relation entre l'exposition aux particules et la mortalité cardio-pulmonaire', Journal of Air and Waste Management Association 51, 203-219, 2001.

[3] Deardorff J W, 'A numerical study of three-dimensional turbulent channel flow at large Reynolds numbers', Journal of Fluid Mechanic, 41, 453-480, 1970.

[4] Hoek G, Brunekreef B, Verhoeff A, van Wijnen J, Fischer P, 'Daily mortality and air pollution in the Netherlands', Journal of the Air and Waste Management Association 50, 1380-1389, 2000.

[5] Lilly D.K, 'On the Application of the Eddy Viscosity Concept in the inertial Sub-range of Turbulence', NCAR Report No. 123, 1966.

[6] Lyn D.A, Rodi W, 'The Flapping Shear Layer Formed by Flow Separation from the Forward Corner of a Square Cylinder', Journal of Fluid Mechanics 267, 353, 1994.

[7] Mavroidis I, Griffiths R.F, Hall D.J, 'Field and Wind Tunnel Investigations of Plume Dispersion around Single Surface Obstacles', Atmospheric Environment 37, 2903–2918, 2003.

[8] Murakami S, Mochida A, 'Three-Dimensional Numerical Simulation of Air Flow around a Cubic Model by Means of Large Eddy Simulation', Journal of Wind Engineering and Industrial Aerodynamics, 25, 291-305, 1987.

[9] Murakami S, Mochida A, '3-D Numerical simulation of the Airflow around a Cubic Model by means of the $\kappa-\varepsilon$ model', Journal of Wind Engineering and Industrial Aerodynamics, 31, 283-303, 1988.

[10] Nyberg F, Gustavsson P, Jarup L, Bellander T, Berglind N, Jackobsson R, Pershagen G, 'Urban air pollution and lung cancer in Stockholm', Epidemiology 11 (5), 487-495, 2000.

[11] Peterka J.A, Meroney R.N, Kothari K.M, 'Wind Flow Patterns about Buildings', Journal of Wind Engineering and Industrial Aerodynamics 21, 21-38, 1985.

[12] Pielke R.A, Nicholls M.E, 'Use of meteorological models in computational wind engineering', Journal of Wind Engineering and Industrial Aerodynamics 67&68, 363-372, 1997.

[13] Rodi W, 'Comparison of LES and RANS calculations of the flow around bluff bodies', Journal of Wind Engineering and Industrial Aerodynamics 69-71, 55 75, 1997.

[14] Rogallo R.S, and Moin P, 'Numerical Simulation of Turbulent Flows', *Ann. Rev. Fluid Mech.,* Vol. 16, pp. 99-137, 1998.

[15] Shah K B, 'Large Eddy Simulation of Flow Past a Cubic Obstacle', PhD Thesis, Stanford University, 1998.

[16] Smagorinsky J, 'General Circulation Experiments with the Primitive Equations I. The Basic Experiment', *Mon. Weather Rev.,* Vol. 91, No. 3, pp. 99-164, 1963.

[17] Vardoulakis S, Fisher B.E.A, Pericleous K, Gonzalez-Flesca N, 'Modeling air quality in street canyons: a review', Atmospheric Environment 37, 155–182, 2003.

[18] Versteeg H.K, Malalasekera W, 'An Introduction to Computational Fluid Dynamics, the Finite Volume Method', Second Edition, Pearson Education Limited 2000.

[19] Wengle H, Werner H, 'Large Eddy Simulation of Turbulent Flow over and around a Cube in a Plate Channel', Eight Symposium on Turbulent Shear Flows, Technical University of Munich, Sep 9-11, 1991.

[20] Zhang Y.Q, Arya S.P, Snyder W.H, 'A Comparison of Numerical and Physical Modeling of Stable Atmospheric Flow and Dispersion around a Cubical Building', Atmospheric Environment Vol. 30, No. 8, pp. 1327-1345, 1996.